Molecular Biology of the Cell
Vol. 8, 2291–2306, November 1997

End4p/Sla2p Interacts with Actin-associated Proteins for Endocytosis in *Saccharomyces cerevisiae*

A. Wesp,* L. Hicke,† J. Palecek,‡ R. Lombardi,* T. Aust,* A.L. Munn,§ and H. Riezman*‖

*Biozentrum of the University of Basel, CH-4056 Basel, Switzerland; †Department of Biochemistry, Molecular Biology and Cell Biology, Northwestern University, Evanston, Illinois; ‡Institut für Biochemie und Molekulare Zellbiologie, University of Vienna, A-1030 Wien, Austria; and §Institute of Molecular Agrobiology, Singapore

Submitted June 4, 1996; Accepted August 6, 1997
Monitoring Editor: Randy Schekman

end4–1 was isolated as a temperature-sensitive endocytosis mutant. We cloned and sequenced *END4* and found that it is identical to *SLA2/MOP2*. This gene is required for growth at high temperature, viability in the absence of Abp1p, polarization of the cortical actin cytoskeleton, and endocytosis. We used a mutational analysis of *END4* to correlate in vivo functions with regions of End4p and we found that two regions of End4p participate in endocytosis but that the talin-like domain of End4p is dispensable. The N-terminal domain of End4p is required for growth at high temperature, endocytosis, and actin organization. A central coiled-coil domain of End4p is necessary for formation of a soluble sedimentable complex. Furthermore, this domain has an endocytic function that is redundant with the function(s) of *ABP1* and *SRV2*. The endocytic function of Abp1p depends on its SH3 domain. In addition we have isolated a recessive negative allele of *SRV2* that is defective for endocytosis. Combined biochemical, functional, and genetic analysis lead us to propose that End4p may mediate endocytosis through interaction with other actin-associated proteins, perhaps Rvs167p, a protein essential for endocytosis.

INTRODUCTION

In *Saccharomyces cerevisiae*, both fluid-phase and receptor-mediated endocytosis are dependent on actin (Kübler and Riezman, 1993). Insight into the mechanism and the requirements of initial endocytic events in yeast has come through the analysis of mutants defective for receptor-mediated endocytosis of the mating pheromone α-factor and fluid-phase endocytosis of Lucifer yellow (LY). Identification of the genes affected in the mutants showed that actin (*END7/ACT1*) and genes that are required for proper actin cytoskeleton organization, such as *END3*, *END4*, *END5*, and *END6* (Bénédetti *et al.*, 1994; Munn *et al.*, 1995) are involved in the internalization step of endocytosis. In addition, mutations affecting other proteins that regulate the integrity of the actin cytoskeleton such as fimbrin, calmodulin, and type I unconventional myosin also block endocytosis (Kübler and Riezman, 1993; Kübler *et al.*, 1994; Geli and Riezman, 1996). Thus, many mutations that disturb the integrity of the actin cytoskeleton affect endocytosis.

In yeast, actin has been localized by indirect immunofluorescence to two distinct structures: actin cables that traverse the mother cell and cortical actin patches that are located at the sites of cell surface growth (Adams and Pringle, 1984). One of the proteins localized to the cortical actin patches is Abp1p, a protein with an SH3 domain (src-homology 3 domain; Drubin *et al.*, 1988; Mulholland *et al.*, 1994). Overexpression of *ABP1* confers loss of polarized growth, delocalized assembly of cortical actin, and inviability at high temperatures (Drubin *et al.*, 1988), whereas deletion of *ABP1* does not produce a detectable phenotype. The mechanism of action on the actin cytoskeleton and the exact function of Abp1p, however, is unknown. Lila

‖ Corresponding author.

© 1997 by The American Society for Cell Biology

and Drubin (1997) demonstrated that Abp1p binds to the SH3 domain of Rvs167p. Rvs167p is homologous to amphiphysin, a protein involved in synaptic membrane recycling (David *et al.*, 1996). Phenotypes of mutations in *RVS167* and a related gene, *RVS161/END6*, are an inability to adapt to unfavorable growth conditions, altered actin organization, and defects in endocytosis (Bauer *et al.*, 1993; Munn *et al.*, 1995; Sivadon *et al.*, 1995). In addition to binding to Rvs167p, Abp1p has been shown to bind, via its SH3 domain, to the proline-rich region of Srv2p in vitro and mediate the cortical actin cytoskeleton localization of Srv2p in vivo (Freeman *et al.*, 1996; Lila and Drubin, 1997). Genetic studies indicate that Srv2p/CAP has at least two independent functions. First, it integrates RAS function through activation of the adenylate cyclase (Fedor-Chaiken *et al.*, 1990; Field *et al.*, 1990; Gerst *et al.*, 1991). Second, Srv2p/CAP regulates the integrity of the actin cytoskeleton, possibly via actin monomer sequestration (Freeman *et al.*, 1995).

To gain more insight into the function of *ABP1*, Holtzman *et al.* (1993) searched for genes that are required for viability in the absence of *ABP1* and thereby identified *SLA2*, a nonessential gene that itself is required for proper organization of the actin cytoskeleton, growth at higher temperatures, and morphogenesis. Sla2p may promote actin polymerization (Li *et al.*, 1995) although how Sla2p exerts this function or other function(s) is unknown.

We show herein that *SLA2* is allelic to *END4*, a gene required for the internalization step of endocytosis (Raths *et al.*, 1993). Amino acid sequence analysis of End4p suggests that it may contain domains that mediate protein–protein interactions. First, End4p contains a proline-rich region. SH3 domains mediate binding to components of the cell cortex (Drubin *et al.*, 1990; Chenevert *et al.*, 1992; Bauer *et al.*, 1993; Holtzman *et al.*, 1993) via proline-rich regions in target proteins (Ren *et al.*, 1993; Freeman *et al.*, 1996). Second, End4p contains a putative coiled-coil region, and coiled-coil domains have repeatedly been found to mediate protein–protein interactions (Crouzet *et al.*, 1991; Bauer *et al.*, 1993; Pollard *et al.*, 1994). Interestingly, a putative leucine-zipper motif is part of the coiled-coil structure. Leucine zippers can serve to form multimeric structures through the interaction of amphipathic helices (Harbury *et al.*, 1993). Third, the C terminus of End4p is homologous to the C terminus of talin (Holtzman *et al.*, 1993). Talin regulates actin dynamics and it connects the actin cytoskeleton to the plasma membrane at adhesion plaques in mammalian cells (Burridge *et al.*, 1988; Muguruma *et al.*, 1990; Rees *et al.*, 1990; Luna, 1991; Turner and Burridge, 1991). Talin and filamentous actin colocalize in macrophages specifically during receptor-mediated phagocytosis (Greenberg *et al.*, 1990; Allen and Aderem, 1995), implicating a role for talin in this process.

We used a mutational analysis of *END4* to correlate in vivo functions with regions of End4p and found that two regions of End4p participate in endocytosis. An N-terminal domain is essential for endocytosis. A central coiled-coil domain, required to form a complex, performs a redundant endocytic function with *ABP1* and *SRV2*. We isolated a novel endocytosis mutant, *srv2–14*, that shows a recessive negative phenotype, and we propose that End4p may mediate endocytosis through the interaction with other actin cytoskeleton-associated proteins.

MATERIALS AND METHODS

Media, Reagents, and Strains

Yeast cells were grown in YPUADT [1% yeast extract, 2% peptone (both Life Technologies, Paisley, Great Britain], 20 mg/l uracil, 20 mg/l adenine, and 20 mg/l tryptophan (E. Merck, Darmstadt, Germany; 2% glucose). Lyticase was prepared as described (Hicke *et al.*, 1997). Chemicals were from Bio-Rad (Richmond, CA), Merck, Fluka (Buchs, Switzerland), or Sigma (St. Louis, MO). F1β and Emp47p antibodies were kindly provided by G. Schatz and S. Schröder, respectively (Biozentrum, Basel, Switzerland). DNA restriction enzymes were purchased either from Boehringer Mannheim (Mannheim, Germany) or New England Biolabs (Beverly, MA). Solid medium contained 2% Bactoagar (Difco, Detroit, MI). 5′ fluoroorotic acid was used at 0.83 mg/ml in synthetic complete medium (Dulic *et al.*, 1991). LY carbohydrazide was obtained from Fluka. Rhodamine-labeled phalloidin was obtained from Sigma. ^{35}S-labeled α-factor was prepared and isolated as described (Dulic *et al.*, 1991). Oligonucleotides were obtained from Microsynth (Balgach, Switzerland). DNA sequencing was performed with a United States Biochemical Sequenase II DNA sequencing kit and polymerase chain reaction (PCR) was carried out by following standard protocols using *Pyrococcus furiosus* (*Pfu*) polymerase. *sla2* strains used for α-factor assays were obtained by crossing *sla2* mutant cells (kindly provided by Dr. D. Drubin, University of California, Berkeley) to either RH732 or RH449 and retaining temperature-sensitive *bar1* segregants. A *Mat***a** *srv2::HIS3 bar1* strain (RH4008) was obtained by crossing DDY952 (*srv2::HIS3*; D. Drubin) to RH3395 and selecting *END4 srv2::HIS3* segregants. Other strains used are described in Table 1.

Cloning of END4 and END14 (SRV2)

The *END4* gene was cloned by complementation of the temperature-sensitive growth phenotype of an *end4–1* strain (RH1597) using a yeast CEN-based genomic library (Rose *et al.*, 1987). The *end4–1* complementing plasmid (pSR2) contained a 16-kb *Sau*3A–*Bam*HI insert. The complementing fragment of pSR2 was further defined and ligated as a 4.4-kb *Xba*I–*Spe*I fragment into linearized YCplac33 at the *Xba*I site to give plasmid pGP6 (Parraga, personal communication). The insert in pGP6 contains only one complete open reading frame (ORF). This plasmid complements the temperature-sensitive phenotype of RH1597 and restores both growth and endocytosis at 37°C in *end4*Δ mutants. Overlapping fragments of pGP6 were cloned into pBSK and used for sequencing. To confirm that the cloned fragment contained the authentic *END4* locus, the chromosomal locus was tagged with *URA3* by cloning the complementing fragment into an *URA3* carrying integration vector followed, by linearizing this plasmid at the *Xho*I site within the putative *END4* ORF and integrating this construct in the wild-type RH449 strain. Uracil prototrophs were crossed to a temperature-sensitive *end4–1* strain (RH1807) and diploids were sporulated and tetrads were dissected as described. We observed tight linkage between uracil prototrophy and temperature-resistant growth, demonstrating that

Table 1. Yeast strains used in this study

Strain	Genotype	Source
RH2887	*Mat***a** *lys2 leu2 ura2 his3 trp1 bar1*	Lab strain
RH2966	*lys2/lys2 leu2/leu2 ura3/ura3 his3/his3 trp1/trp1 bar1/bar1*	Lab strain
RH449	*Matα his4 lys2 leu2 ura3 bar1*	Lab strain
RH732	*Mat***a** *his4 lys2 leu2 ura3 bar1 pep4::URA3*	Lab strain
RH2635	*Matα his4 leu2 ura3 bar1*	Lab strain
RH977	*Matα his4 leu2 ura3 trp1::URA3*	Lab strain
RH978	*Mat***a** *his4 leu2 ura3 trp1::URA3*	Lab strain
RH2974	*his3/his3 trp1/trp1 lys2/lys2 ura3/ura3 leu2/leu2 bar1/bar1 END4/end4::HIS3*	This study
RH3391	*Mat***a** *his3 lys2 ura3 leu2 trp1 bar1 end4::HIS3* p[*END4; URA3*]	This study
RH3297	*Mat***a** *his3 lys2 ura3 leu2 trp1 bar1 abp1::URA3*	This study
RH2763	*Mat***a** *his4 leu2 ura3 bar1 pep4::URA3 sla2-1*	This study
RH2764	*Mat***a** *leu2 ura3 lys2 bar1 pep4::URA3 sla2-2*	This study
RH2765	*Mat***a** *his4 leu2 ura3 lys2 bar1 sla2-3*	This study
RH2766	*Mat***a** *leu2 ura3 lys2 bar1 pep4::URA3 sla2-4*	This study
RH2767	*Mat***a** *leu2 ura3 lys2 bar1 pep4::URA3 sla2-5*	This study
RH1597	*Mat***a** *lys2 leu2 ura3 his4 bar1 end4-1* (*sla2-41*)	Raths *et al.* (1993)
Rh1807	*Mat***a** *ura3 his4 pep4 bar1 end4-1* (*sla2-4*)	Lab strain
Rh3393	*Mat***a** *lys2 leu2 ura3 his3 bar1 end4::HIS3 END4:TRP1*	This study
RH3395	*Mat***a** *lys2 leu2 ura3 his3 bar1 end4::HIS3 end4Δ376-501:TRP1*	This study
RH3397	*Mat***a** *lys2 leu2 ura3 his3 bar1 end4::HIS3 end4Δ495-573:TRP1*	This study
RH3399	*Mat***a** *lys2 leu2 ura3 his3 bar1 end4::HIS3 end4Δ376-573:TRP1*	This study
RH3401	*Mat***a** *lys2 leu2 ura3 his3 bar1 end4::HIS3 end4Δ376-440:TRP1*	This study
RH3403	*Mat***a** *lys2 leu2 ura3 his3 bar1 end4::HIS3 end4Δ286-301:TRP1*	This study
RH3769	*Mat***a** *lys2 leu2 ura3 his3 bar1 end4::HIS3 end4Δ114-284:TRP1*	This study
RH3771	*Mat***a** *lys2 leu2 ura3 his3 bar1 end4::HIS3 end4Δ318-373:TRP1*	This study
RH3295	*Mat***a** *his3 lys2 ura3 leu2 bar1 end4::HIS3 end4Δtalin:TRP1*	This study
RH3405	*Mat***a** *lys2 leu2 ura3 his3 bar1 end4::HIS3 END4:TRP1 abp1::URA3*	This study
RH3407	*Mat***a** *lys2 leu2 ura3 his3 bar1 end4::HIS3 end4Δ376-501:TRP1 abp1::URA3*	This study
RH3409	*Mat***a** *lys2 leu2 ura3 his3 bar1 end4::HIS3 end4Δ495-573:TRP1 abp1::URA3*	This study
RH3411	*Mat***a** *lys2 leu2 ura3 his3 bar1 end4::HIS3 end4Δ376-573:TRP1 abp1::URA3*	This study
RH3413	*Mat***a** *lys2 leu2 ura3 his3 bar1 end4::HIS3 end4Δ286-301:TRP1 abp1::URA3*	This study
Rh4007	*Mat***a** *lys2 leu2 ura3 his3 bar1 end4::HIS3 end4Δ318-373:TRP1 abp1::URA3*	This study
RH3296	*Mat***a** *his3 lys2 ura3 leu2 bar1 end4::HIS3 end4Δtalin:TRP1abp1::URA3*	This study
RH3993	*Mat***a** *his4 leu2 ura3 end14-1* (*srv2-14*)	This study
RH4008	*Mat***a** *his3 leu2 ura3 lys2 bar1 srv2::HIS3*	This study
RH4009	*Mat***a** *lys2 leu2 ura3 his3 bar1 end4::HIS3 end4Δ376-501:TRP1srv2::URA3*	This study
L40	*Mat***a** *his3 trp1 leu2 ade2 lexA-HIS3:LYS2 lexA-lacZ:URA3 gal4*	Fields *et al.* (1994)

the cloned locus in pGP6 indeed corresponds to the authentic *END4* locus. An ~4.2-kb *Bam*HI–*Hin*dIII *END4*-containing fragment was ligated into high-copy-number vector YEplac181 to overexpress *END4*.

The *END14* gene was cloned by complementation of the temperature-sensitive growth phenotype of an *end14–1* strain (RH3993) using a yeast CEN-based genomic library (Munn *et al.*, 1995). The *end14–1* complementing fragment was found to reside within a 3.3-kb *Bam*HI–*Hin*dIII fragment, which was cloned into YCplac111 to give pTA2 and cloned into YIplac128 to give pTA3. DNA sequencing revealed that *SRV2* is the only ORF on this fragment. pTA3 was linearized using the unique restriction site *Stu*I within the ORF of *SRV2* and then transformed into wild-type RH977 strain to mark this locus with *LEU2*. Leucine prototrophs were then crossed to temperature-sensitive *end14–1* strains and diploids were sporulated and dissected. In 48 dissected tetrads, leucine prototrophs were always temperature-resistant for growth showing that *end14–1* is allelic to *SRV2*.

Deletion of END4 and END14 (SRV2)

All *END4*-containing plasmids were derived from pGP6. Plasmid pWA4 was constructed by ligating the ~4.2-kb *Bam*HI–*Hin*dIII fragment from pGP6 into pBSK− linearized with *Bam*HI/*Hin*dIII. The complete *END4* ORF including 135 nucleotides upstream and 65 nucleotides downstream were replaced by a 1.2-kb *Bam*HI fragment containing the *HIS3* ORF. This did not affect adjacent ORFs (Yeast Genome Project, final release of the complete genome on April 24, 1996. http://speedy.mips.biochem.mpg.de/mips/yeast). The resulting plasmid pWA9 was digested with *Eco*RI and the *HIS3*-containing 2.4-kb fragment was transformed into RH2966 for integration/replacement of *END4*, generating RH2974. Transformants were selected on minimal medium lacking histidine. Diploids were transformed with pGP6 to increase *end4*Δ spore viability, sporulated, and dissected as described. Deletion of only one copy of *END4* was confirmed by tetrad analysis. Correct integration replacement of *END4* was confirmed by the lack of End4p in total protein extracts of histidine prototrophic segregants of RH2974.

END14 was deleted by integration replacement. A *URA3*-containing PCR fragment was generated using pRS416 (Sikorski and Hieter, 1989) as a template with primers having homology to the 5′ and 3′ sequences of *END14* (Lila and Drubin, 1997). Correct integration in diploid transformants prototrophic for uracil was confirmed by PCR analysis (our unpublished results).

Construction of Mutant end4 Alleles

All mutant *end4* alleles were cloned into the yeast integration vector pRS404 carrying *TRP1* as a selectable marker (kindly provided by

Dr. P. Phillippsen, Biocenter, Basel, Switzerland). In all cases the *Hin*dIII site in the polylinker was eliminated either by inserting mutant *end4* alleles or by specific elimination of the site (generating pRS404′) prior to insertion of mutant *end4* alleles. After cloning of mutant *end4* alleles into this integration vector, the only *Hin*dIII site left was within the *TRP1* sequence. To delete the End4p talin-like C-terminal domain, two complementary oligonucleotides encoding three consecutive stop codons were hybridized and blunt-end ligated into the *END4* coding sequence at the *Hin*cII restriction site. This introduces in-frame stop codons just after amino acid 766. The resulting allele was named *end4Δtalin*. To facilitate generation of *end4* deletion constructs, we introduced an artificial *Stu*I site into *END4*. This results in two changes in the amino acid sequence of End4p (A642V/I643L). Introduction of the unique *Stu*I site was confirmed by DNA sequencing, and we showed that the introduced changes in the protein sequence of End4p does not interfere with *END4* function (see RESULTS). An ~4.2-kb *END4 Bam*HI–*Hin*dIII fragment containing the *Stu*I site was cloned into pRS404′ at the *Spe*I site to give plasmid pWA27. Subsequent *end4* alleles were derived from pWA27 as follows: the ~800-bp *END4 Xho*I–*Stu*I fragment of pWA27 was replaced with PCR-generated *Xho*I–*Stu*I fragments that lacked various domains of the wild-type fragment. Alleles were named as follows (deleted amino acids in parentheses): *end4Δcoil1* (376–501), *end4Δcoil2* (495–573), *end4Δcoil1,2* (376–573), and *end4ΔGln* (376–440). The proline-rich sequence in *END4* (amino acids [aa] 286–301) was deleted using a two-step PCR generating an ~670-bp *Kpn*I–*Xho*I fragment. This fragment was used to replace the *Kpn*I–*Xho*I fragment of *END4* to generate *end4Δ286–301*, which is referred to as *end4ΔPro*. The N-terminal deletion alleles were constructed as follows: a one-step PCR yielded the *Kpn*I–*Xho*I fragments containing *end4Δ114–284* and *end4Δ318–373*, respectively, which were used to replace the *Kpn*I–*Xho*I fragment of *END4*.

In-frame deletions of the *END4* gene created by PCR were confirmed by sequencing the relevant regions. All newly generated *end4* alleles, and the wild-type *END4* gene, were subcloned into *TRP1*-marked integration vectors. The resulting constructs, linearized with *Hin*dIII, were integrated at the *trp1* locus of diploid RH2974. Integrants were selected by growth at 24°C on synthetic medium lacking tryptophan, restreaked for single colonies, then sporulated, and dissected as described below. Segregants prototrophic for both histidine and tryptophan were selected. Integration at *trp1* was verified by crossing these segregants to RH2635. All segregants of the resulting diploids were prototrophic for tryptophan, confirming integration of the mutant *end4* alleles at the *trp1* locus. Expression of mutant End4p and concomitant lack of wild-type End4p was confirmed by immunodetection of End4p in total protein extracts prepared from His+ Trp+ segregants.

Endocytosis Assays

Pheromone-uptake assays were performed using a continuous presence protocol as described earlier (Dulic *et al.*, 1991). Cultures were grown at 24°C to 0.5–1.5 × 10^7 cells/ml, and the cells were harvested by centrifugation at 3000 rpm for 5 min in a GLC (General Laboratory Centrifuge, Sorvall, Lausanne, Switzerland) in 50-ml Falcon tubes. Cells were then resuspended in YPUADT at 2–3 × 10^8 cells/ml and incubated at the respective growth temperature for 5 min on a rotary aquashaker (Kühner, Basel, Switzerland). Then ^{35}S-labeled α-factor was added and samples were taken at the indicated time points after α-factor addition. Cells were diluted 1:100 into ice-cold pH 1 (50 mM sodium citrate) or pH 6 (50 mM potassium phosphate) buffer. The pH 6 samples were filtered immediately onto GF/C filters (Whatman, Maidstone, England) on a vacuum pump, whereas the pH 1 samples were kept on ice for 20 min prior to filtering. Filters were washed with ice-cold buffer, transferred to 20-ml screw-cap polyethylene scintillation vials (Packard, Meriden, CT), and dried at 80°C for 15 min before adding 5 ml of emulsifier-safe scintillation cocktail (Packard). The radioactivity associated with each cell sample was measured in a β-counter (1900 TR, Packard). The percentage of internalized α-factor was calculated as follows: 100 × cpm(pH 1)/cpm(pH 6). Endocytic rates were determined as the slope of the internalization curves within the range of 5 to 15 min, using the linear regression curve fitting option on a HP48SX calculator, thus expressing percentage of internalized ligand per minute.

LY accumulation was assayed as described in Munn *et al.* (1995).

Generation of Antibodies, Protein Extracts, and Immunoblot Analysis

Antibodies against End4p were raised in female New Zealand White rabbits using the extreme N-terminal peptide (SRIDSDLQKALKK) and the extreme C-terminal peptide (KRLGEIRRHAYYNQDDD) as described (Harlow and Lane, 1988). Protein extracts were prepared as described (Horvath and Riezman, 1994). Protein extracts dissolved in sample buffer were separated on denaturing SDS-PAGE minigels (Hoefer Scientific Instruments, San Francisco, CA) and transferred to nitrocellulose filters as described (Schimmöller *et al.*, 1995). Molecular weight markers were purchased from Bio-Rad. Nitrocellulose membranes were incubated for 30 min at room temperature (RT) in blocking buffer [0.1 M NaCl, 80 mM Na_2HPO_4, 20 mM NaH_2PO_4, 2% (wt/vol) nonfat-dry milk, 0.1% Nonidet P-40]. Antibodies were added in fresh buffer and incubation was continued either at RT for 1.5 h or at 4°C overnight; filters were subsequently washed three times with blocking buffer and three times with PBS (0.1 M NaCl, 80 mM Na_2HPO_4, 20 mM NaH_2PO_4). Then, goat anti-rabbit IgG coupled to horseradish peroxidase (Sigma) was added at a dilution of 1:8000 and incubation was continued for 1 h at RT before filters were washed as described above. Antibody conjugates were visualized using the ECL detection kit (Amersham) and Kodak XAR-5 film. Quantifications were carried out using densitometric scanning (Molecular Dynamics, Sunnyvale, CA).

Preparation of Spheroplasts and Cell Fractionation

Cultures were grown to 2–5 × 10^7 cells/ml and then the cells were harvested in GSA bottles by centrifugation at 5000 rpm for 5 min (Sorvall, RC2-B). The cells were resuspended in 0.1 M Tris sulfate (pH 9.4), and 28 mM 2-mercaptoethanol, transferred to 50-ml Falcon tubes (Becton Dickinson, Franklin Lakes, NJ), and incubated at RT with slow shaking for 20 min (100 ml of buffer per 2–10 × 10^{10} cells). Cells were pelleted in a Sorvall GLC at 3000 rpm for 5 min, resuspended in 20 ml of 2% yeast extract, 1% peptone, 10 mM Tris (pH 8), and 0.7 M sorbitol containing lyticase (0.01–0.02 mg/ml) and incubated at 30°C on a rotary aquashaker at 100 rpm until >90% of the cells lysed upon osmotic shock. To check for lysis, an aliquot was diluted in 20 mM NaCl, 10 mM Tris, pH 8, and 5 mM $MgCl_2$ and observed under the microscope. Yeast cells were fractionated according to a modified version of the method of Pryer *et al.* (1993). Spheroplasts were washed once in 0.1 M NaCl, 10 mM Tris, pH 8, 5 mM $MgCl_2$, and 0.7 M sorbitol, resuspended in 2 ml of lysis buffer (0.1 M NaCl, 20 mM 2-(N-morpholino)ethane-sulfonic acid (MES) pH 6.5, 5 mM $MgCl_2$) containing leupeptin (1 μg/ml), aprotinin (1 μg/ml), and pepstatin (1 μg/ml) to 2–5 × 10^9 cells/ml, and lysed on ice by douncing with 36 strokes in a 5-ml Dounce homogenizer (Wheaton, Dietikon, Switzerland). The lysate was centrifuged at 1000 × *g* for 5 min at 4°C in a tabletop centrifuge (Heraeus, Sepatech, Switzerland) to remove unbroken cells and large cell debris. Then, equal volumes (0.1 ml) of supernatant and reagents in lysis buffer were mixed to give final reagent concentrations of 1% Triton X-100, 0.5 M NaCl, 2.5 M urea, or 0.1 M Na_2CO_3 (pH 11.5), and incubated for 1 h on ice. Samples were centrifuged for 1 h at 55,000 rpm in a Beckman TLA100.3 rotor. Pellets and supernatants were denatured in SDS sample buffer and equivalent amounts were

electrophoresed on SDS gels and analyzed by immunoblotting as described.

According to *k*-value calculations, one half of the total amount of a particle of about 9.1 S will sediment in 1 h of centrifugation at 55,000 rpm in a total volume of 0.2 ml in a TLA100.3 rotor (Beckman). If the particle has a sedimentation value of 8.3 S (estimation for End4Δcoil1p homodimers is around 210 kDa) about 45% would be recovered under the same centrifugation conditions in the pellet fraction.

Sucrose Velocity Gradients

Wild-type RH732 cells were grown at 24°C to 2–5 × 10^7 cells/ml and 4–10 × 10^{10} cells were converted to spheroplasts as described above. Spheroplasts were washed once in 150 mM potassium acetate, 20 mM HEPES (pH 6.8), and 5 mM magnesium acetate containing 0.7 M sorbitol for osmotic support and resuspended in ice-cold lysis buffer (20 mM NaCl, 10 mM Tris-Cl, pH 8, 5 mM $MgCl_2$) containing leupeptin (1 μg/ml), aprotinin (1 μg/ml), and pepstatin (1 μg/ml) to 2–5 × 10^9 cells/ml. Phenylmethylsulfonyl fluoride (100 mM stock in isopropanol) was added to a final concentration of 1 mM, and spheroplasts were lysed by 48 strokes on ice in a 5-ml Dounce homogenizer (Wheaton). The lysate was centrifuged at 1000 × *g* for 1 min in a tabletop centrifuge (Heraeus) to remove unbroken cells. Then, the supernatant was further centrifuged at 1000 × *g* for 3 min to give P1 and S1. S1 (560 μl) was mixed with 140 μl of 150 mM potassium acetate, 20 mM HEPES (pH 6.8) and 5 mM magnesium acetate containing 20% Triton X-100 and incubated for 20 min at RT before loading the entire volume onto preformed sucrose gradients. Centrifugation was carried out for 18 to 19 h at 4°C in a Centrikon TST41.14 rotor at 130,000 × *g* (32,000 rpm, Kontron TGA-65 ultracentrifuge, Zurich, Switzerland) and was terminated without brakes. The gradients were prepared as follows: 1.875-ml volumes of 30%, 25%, 21%, 17%, 13%, 9% sucrose (wt/vol) in 150 mM potassium acetate, 20 mM HEPES (pH 6.8), and 5 mM magnesium acetate containing 1% Triton X-100 were layered on top of each other in 13-ml plastic tubes (Beckman ultra-clear tubes, 14 × 89 mm) and stored overnight at 4°C. Fractions of 320 μl each were collected from the top of the gradient with a Gilson P1000 pipette. Pellets were resuspended in 1% SDS, and equal amounts were loaded onto SDS gels. Proteins were transferred to nitrocellulose filters and detected as described. Sucrose (as percent wt/vol) was determined by measuring refractive indices and reading values from a standard curve. Total protein was determined using the BCA kit (Pierce, Rockford, IL). Markers used were bovine serum albumin (66 kDa, Sigma), aldolase (147 kDa), β-amylase (200 kDa, Sigma), catalase (232 kDa, Sigma), and apoferritin (443 kDa, Sigma). Each marker (0.7 mg) was loaded and fractions were collected as described. Calculations according to Griffith (1979) were carried out to determine the molecular weight of the End4p-containing complex (corrected for water at 20°C). Comparison of the End4p-containing complex with a standard curve derived from the markers yielded a molecular weight of the End4p complex of 222 ± 28 kDa (n = 5).

Two-Hybrid Analysis

For analysis of End4p protein interactions, the entire coding region of *END4* was amplified by PCR using primers introducing *Bam*HI sites 2 bp upstream of the initiator methionine and downstream of the last codon, respectively, using pGP6 as a template. This PCR product was digested with *Bam*HI, gel purified, and ligated into *Bam*HI-digested dephosphorylated vector pGAD424 (Fields and Sternglanz, 1994) to give plasmid pGCE, containing the gal4 DNA-activating domain fused to End4p. pGCE complements the growth defect of *end4*Δ mutants at 37°C (our unpublished results). Fusion of the gal4 transcription-activating domain to mutant *end4* alleles was carried out using the same primers as for the full-length *END4* with plasmids containing *end4*Δ*coil1* and *end4*Δ*coil2* alleles to give plasmids pGLE and pGSE, respectively. aa 318–590 of End4p fused to the gal4 transcription-activating domain was isolated during a screen of *RPG1*-interacting proteins (Palecek, unpublished observation). The *Bam*HI fragment of pGCE containing the entire *END4* sequence was cloned into the *Bam*HI site of pBTM116 to give plasmid pLCE, containing an in-frame fusion of the lexA DNA-binding domain and End4p proteins. Yeast strain L40 containing two reporter genes (*lexA-LacZ* and *lexA-HIS3*) was transformed with pLCE and the plasmids containing the various DNA-activating domain fusion proteins. Histidine prototrophy was scored on plates containing 0.67% yeast nitrogen base and 2% glucose supplemented with 1 mM 3-amino-1,2,4-triazol after 3 d at 30°C. LacZ enzymic activity was measured as described in Miller (1972). β-Galactosidase activities are expressed as units/milligram of protein.

Miscellaneous

Mating of haploid strains of yeast, sporulation of diploids, and tetrad analysis were performed as described in Sherman *et al.* (1974). Transformation of yeast with plasmid DNA and all DNA manipulations were done as described in Munn *et al.* (1995). Recovery of DNA fragments was performed as described (Sambrook *et al.*, 1989) with DEAE membranes. The End4p protein sequence was analyzed using the University of Wisconsin GCG programs run on a VAX/VMS computer system. Proline at position 498 caused the structure prediction program to divide the region from aa 376 to aa 573 into two separate coiled-coil domains. Actin was stained with rhodamine-coupled phalloidin as described in Munn *et al.* (1995). Carboxypeptidase Y (CPY) metabolic labeling experiments were carried out as described in Mulholland *et al.*, (1997) using a 5-min pulse prior to chase at the indicated time points after 15 min of preincubation at either 24°C or 37°C, respectively.

RESULTS

END4 Is Essential for Endocytosis

end4 mutants were isolated independently in two separate screens for endocytosis mutants and in both cases the mutants were temperature-sensitive for growth (Raths *et al.*, 1993; Munn *et al.*, 1995). We cloned the wild-type *END4* gene by phenotypic complementation of the temperature-sensitive growth defect of an *end4–1* strain and found that *END4* is identical to *SLA2/MOP2*. *SLA2* was isolated because it is essential for viability in the absence of *ABP1*. Sla2p is required for growth at high temperature, viability with *abp1*Δ, and polarization of the cortical actin cytoskeleton (Holtzman *et al.*, 1993). *MOP2* was isolated as a regulator of the abundance of the plasma membrane ATPase at the cell surface (Na *et al.*, 1995). Henceforth we refer to *SLA2/MOP2* as *END4*.

To create a null allele, *END4* was disrupted in a diploid wild-type strain by integration replacement (Figure 1A). We noticed that *end4*Δ segregants were hardly recovered, suggesting that *END4* may be essential for germination and/or growth in our strain background. Therefore, the heterozygous disrupted strain was transformed with a plasmid carrying the wild-type *END4* gene on a centromeric plasmid (pGP6), sporulated, and dissected. *end4*Δ segregants carrying pGP6 were cured of the plasmid at 24°C. Deletion of *END4* was confirmed by the lack of the gene product in plasmid-cured segregants prototro-

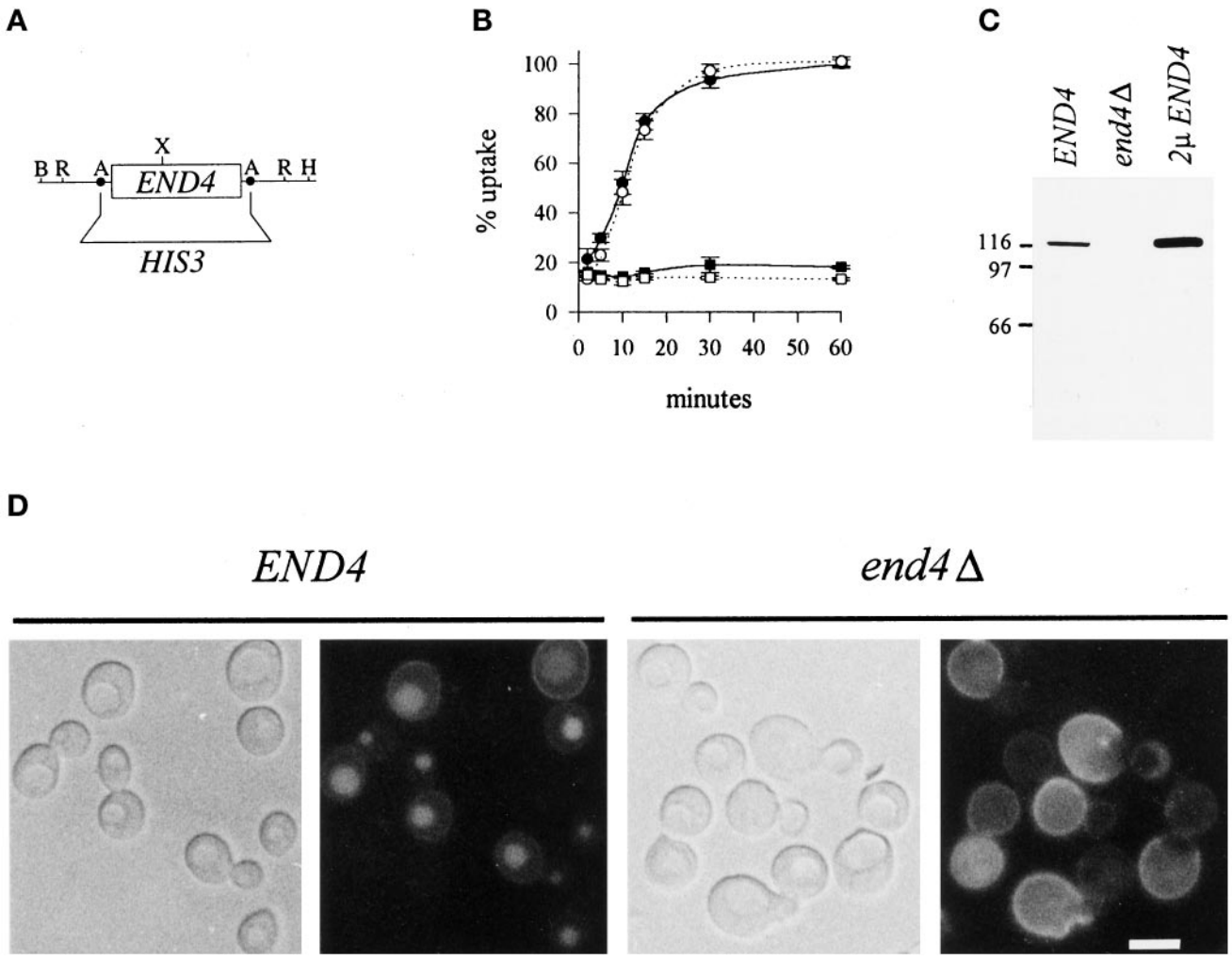

Figure 1. Deletion of *END4* constitutively blocks endocytosis. (A) The complete *END4* ORF on an *Aat*II fragment was replaced with the prototrophic marker *HIS3*. The resulting *Eco*RI fragment was used to delete *END4* by integration/replacement. B, *Bam*HI; R, *Eco*RI; A, *Aat*II; X, *Xho*I; H, *Hin*dIII. (B) Receptor-mediated internalization of α-factor is blocked at both 24°C (solid symbols) and 37°C (open symbols) in RH3391 cells cured of pGP6 (*end4*Δ, squares), whereas RH3393 cells (*END4*, circles) show no defect at either temperature. (C) End4p-specific antiserum generated against a C-terminal peptide specifically recognizes a single band with an apparent mobility of ~116 kDa that is absent in strain RH3391 cured of pGP6 (*end4*Δ) extracts but more prominent in extracts prepared from strains expressing multiple copies of the gene (2μ*END4*). (D) In contrast to strain RH2887 (*END4*), strain RH3391 cured of pGP6 (*end4*Δ) does not accumulate LY in the vacuole after incubation with the dye at 24°C for 1 h. Bar, 5 μm.

phic for histidine (Figure 1C). Growth of *end4*Δ strains at 37°C, but not at 24°C, depended on the presence of pGP6. Thus, deletion of *END4* confers a temperature-sensitive growth phenotype (see Figure 3B) and it may interfere with germination. This may explain why Na *et al.* (1995) reported that *MOP2* is essential for viability. In our background, a null allele results in vegetative growth phenotypes similar to the results described by Holtzman *et al.* (1993).

The originally isolated *end4* alleles showed temperature-sensitive endocytosis, partially defective at 24°C and completely defective at 37°C. To determine whether deletion of the *END4* gene abolishes endocytosis, we assayed fluid-phase endocytosis of LY and receptor-mediated endocytosis of α-factor in *end4*Δ mutants. Cells were grown at 24°C and radiolabeled α-factor was added to cells after a 5-min incubation either at 24°C or 37°C. The percentage of internalized pheromone at each time point was determined by dividing internal (pH 1 resistant) counts by total cell-associated (pH 6 resistant) counts. Wild-type cells internalized α-factor rapidly, irrespective of the temperature of incubation (Figure 1B). In contrast, disruption of the *END4* gene resulted in a complete loss of pheromone internalization at both 24°C and 37°C (Figure

1B). Since *end4*Δ cells were also defective for LY accumulation in the vacuole at 24°C (Figure 1D), we conclude that *END4* is essential for both fluid-phase and receptor-mediated endocytosis. We also found that the five previously isolated temperature-sensitive *sla2* alleles (Holtzman *et al.*, 1993) all showed a defect in α-factor internalization at the restrictive, but not at the permissive, temperature for growth (our unpublished observations). Thus, the independently isolated *end4* and *sla2* alleles are true temperature-sensitive loss of function mutations.

The Coiled-Coil Domain of End4p Is Necessary for Protein Interaction

Antibodies generated against a C-terminal peptide of End4p recognized a single protein in yeast lysates with an apparent molecular weight of about 116 kDa as determined by denaturing SDS-PAGE (Figure 1C). This band was absent in extracts prepared from *end4*Δ strains but was much stronger in extracts from strains carrying the *END4* gene on a high-copy-number plasmid. The fact that End4p migrates more slowly than predicted from its size (109 kDa) may indicate that the protein adopts a special conformation resistant to SDS denaturation or that the protein is posttranslationally modified. To determine whether End4p is soluble or membrane-associated, we incubated wild-type cell extracts with detergent, high salt, urea, or carbonate as described in Figure 2A. After a 1-h high-speed centrifugation, pellets and supernatants were analyzed by immunodetection for End4p, Emp47p, and F1β content. The integral membrane protein Emp47p (Schröder *et al.*, 1995) was only solubilized by treatment of lysates with detergent, whereas a peripheral membrane protein, the F1β subunit of the mitochondrial ATP synthase, was also solubilized by treatment with high salt, urea, and carbonate (Figure 2A). End4p distributed almost equally between the soluble and particulate fraction and treatment of the lysate with detergent did not alter this distribution (Figure 2A). This demonstrates that End4p is not a transmembrane protein but partitions into the particulate fraction as a proteinaceous complex. Consistent with this idea, incubation of cell extracts with agents that disrupt protein–protein interactions solubilized End4p.

The fractionation results suggested that End4p may exist in two forms, one soluble (and not sedimentable) and the other part of a sedimentable complex. To address this question, we analyzed wild-type lysates using velocity centrifugation on linear sucrose gradients. This method allows to resolve (putative) multiple species of End4p. As shown in Figure 2B, End4p was recovered from the gradient as a single peak. The sedimentation coefficient of proteins comigrating with End4p is 10.6 ± 0.8S (Griffith, 1979), which corresponds to an apparent molecular weight of 220 ± 30 kDa, if a globular shape is assumed. As End4p is predicted to have a molecular weight of 109 kDa, the protein most likely exists in a complex, possibly as an End4p homodimer or associated with other protein(s). Because End4p has a predicted coiled-coil structure, it is possible that the protein adopts a nonglobular shape that would cause it to sediment more slowly on velocity gradients. In this case, 220 kDa would be an underestimate of the molecular weight of the complex. The apparent discrepancy between the results from the differential centrifugation and velocity sedimentation experiments can be easily explained. Fifty percent of a 9.1S complex would have sedimented in 1 h under our conditions for differential centrifugation (see MATERIALS AND METHODS).

The middle part of End4p (aa 376–573) has the potential to form a coiled-coil structure (MATERIALS AND METHODS), and it has been reported previously that coiled-coil domains mediate protein–protein interactions (Crouzet *et al.*, 1991; Bauer *et al.*, 1993; Pollard *et al.*, 1994). In light of our results from the fractionation and sedimentation analysis, we tested whether the coiled-coil domain of End4p can mediate End4p–End4p interaction using the two-hybrid system (Fields and Sternglanz, 1994). We therefore created fusion proteins of full-length End4p (or mutant *end4* alleles) with the gal4 transcription-activating domain and tested for interaction with full-length End4p. We found that full-length End4p interacts with itself in the two-hybrid system (Figure 2C) and this interaction depends on the presence of the coiled-coil domain of End4p (aa 376–573). Moreover, this coiled-coil domain itself is sufficient to mediate interaction with End4p in the two-hybrid system. An End4p fragment consisting of aa 318–376 did not interact with full-length End4p in the two-hybrid system (Palecek, unpublished observation). Thus, it is likely that the coiled-coil domain of End4p mediates partitioning of End4p into a sedimentable complex. Consistent with this, sedimentation of End4p upon high-speed centrifugation depends on the presence of the coiled-coil domain (Figure 2, A and D). These results are consistent with the idea that End4p homodimer formation via its coiled-coil domain may be a prerequisite for End4p sedimentation. Alternatively, the coiled-coil domain may mediate interaction with other protein(s) than End4p and dimerization may not be required for association with the sedimentable complex.

The N-terminal Domain of End4p Is Essential for Endocytosis and Actin Organization

Analysis of the End4p amino acid sequence suggests that several regions could be important for the function of the protein (Holtzman *et al.*, 1993; see MATERIALS AND METHODS). These include sequences rich in prolines, glutamines, and the putative coiled-

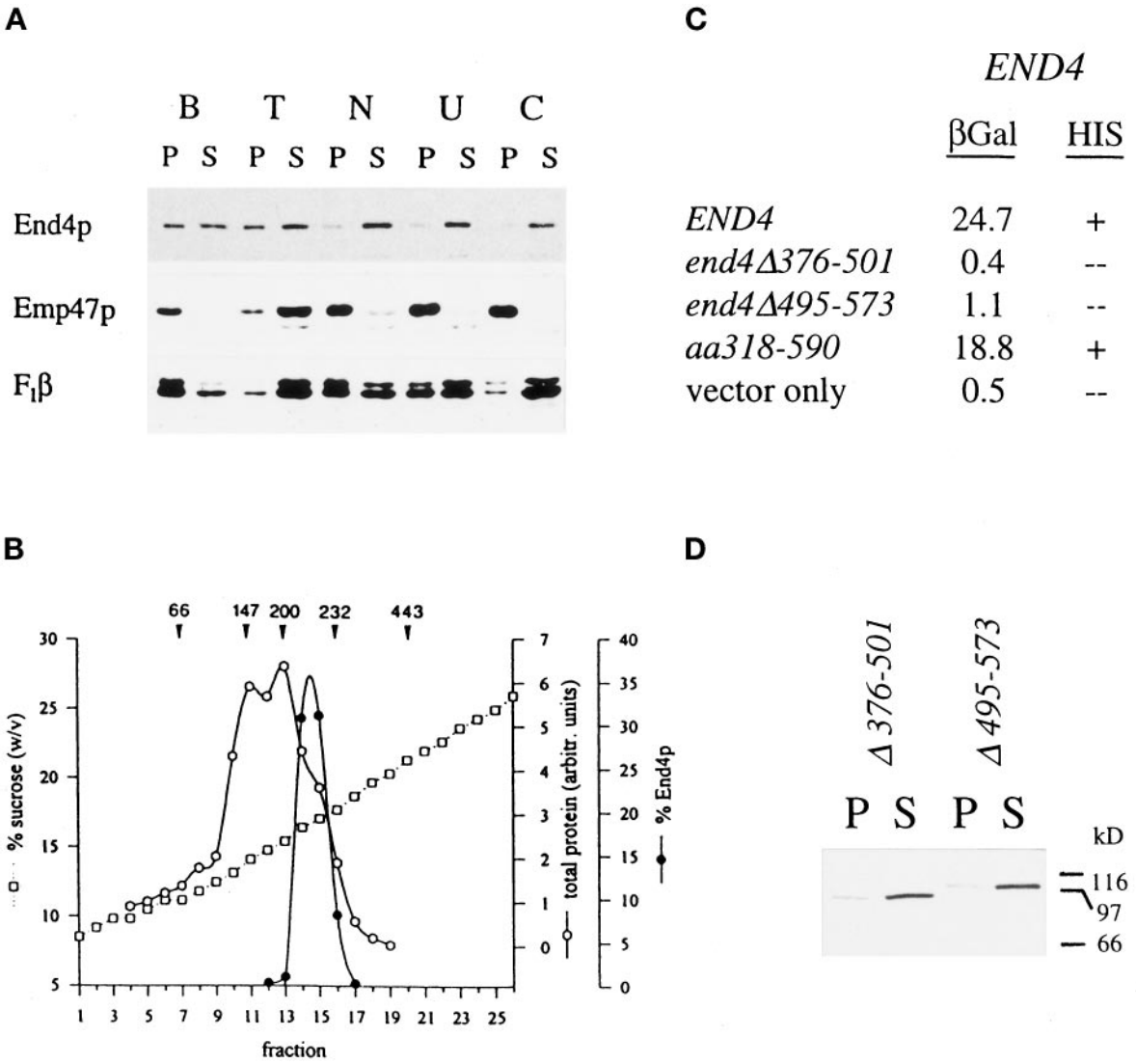

Figure 2. Coiled-coil domain of End4p mediates complex formation. (A) Wild-type cell extracts were incubated on ice for 1 h in 1% Triton X-100 (lane T), 0.5 M NaCl (lane N), 2.5 M urea (lane U), or 0.1 M carbonate, pH 11.5 (lane C) or were mock treated with lysis buffer (lane B). After high-speed centrifugation, equivalent volumes of pellets (lanes P) and supernatants (lanes S) were analyzed for End4p and control proteins by immunodetection. (B) Wild-type cell lysates were fractionated on linear 9–30% sucrose gradients. Fractions were collected from the top (fraction 1) and End4p content was quantified by Western blotting. Arrowheads indicate the position of the peaks of marker proteins; numbers are given in kDa. (C) Wild-type *END4* as well as mutant *end4* alleles were fused in-frame to the gal4 transcription-activation domain. These fusion constructs were tested in the two-hybrid system for interaction with the wild-type *END4* gene fused to the LexA DNA-binding domain. β-Galactosidase activities of extracts prepared from yeast strain L40 harboring the various combinations of plasmids were measured and expressed as units/milligram of protein. Alternatively, growth on plates lacking histidine was scored to monitor interaction of End4p. (D) Extracts of *end4Δ376–501* (RH3395) and *end4Δ495–573* (RH3397) mutants were prepared in lysis buffer and processed as described in A. Mutant End4p was visualized in pellets (lanes P) and supernatants (lanes S) by immunodetection.

coil domain. In addition, the C terminus of End4p has homology to talin (Holtzman *et al.*, 1993), a protein that connects the actin cytoskeleton to membranes in mammalian cells (Rees *et al.*, 1990). To investigate possible in vivo functions mediated by those sequences, we generated *end4* mutants carrying deletions of the above-mentioned regions. In particular, we wanted to know whether the endocytic function of *END4* can be separated from its function in actin cytoskeleton organization and from its growth requirement in an *abp1*Δ background. A schematic overview of the *end4* deletion alleles is given in Figure 3A. Mutant *end4* alleles were integrated (expressed from the wild-type promoter) in an *end4*Δ background and we then determined whether they could rescue the multiple defects of the *end4* null mutant. All mutant

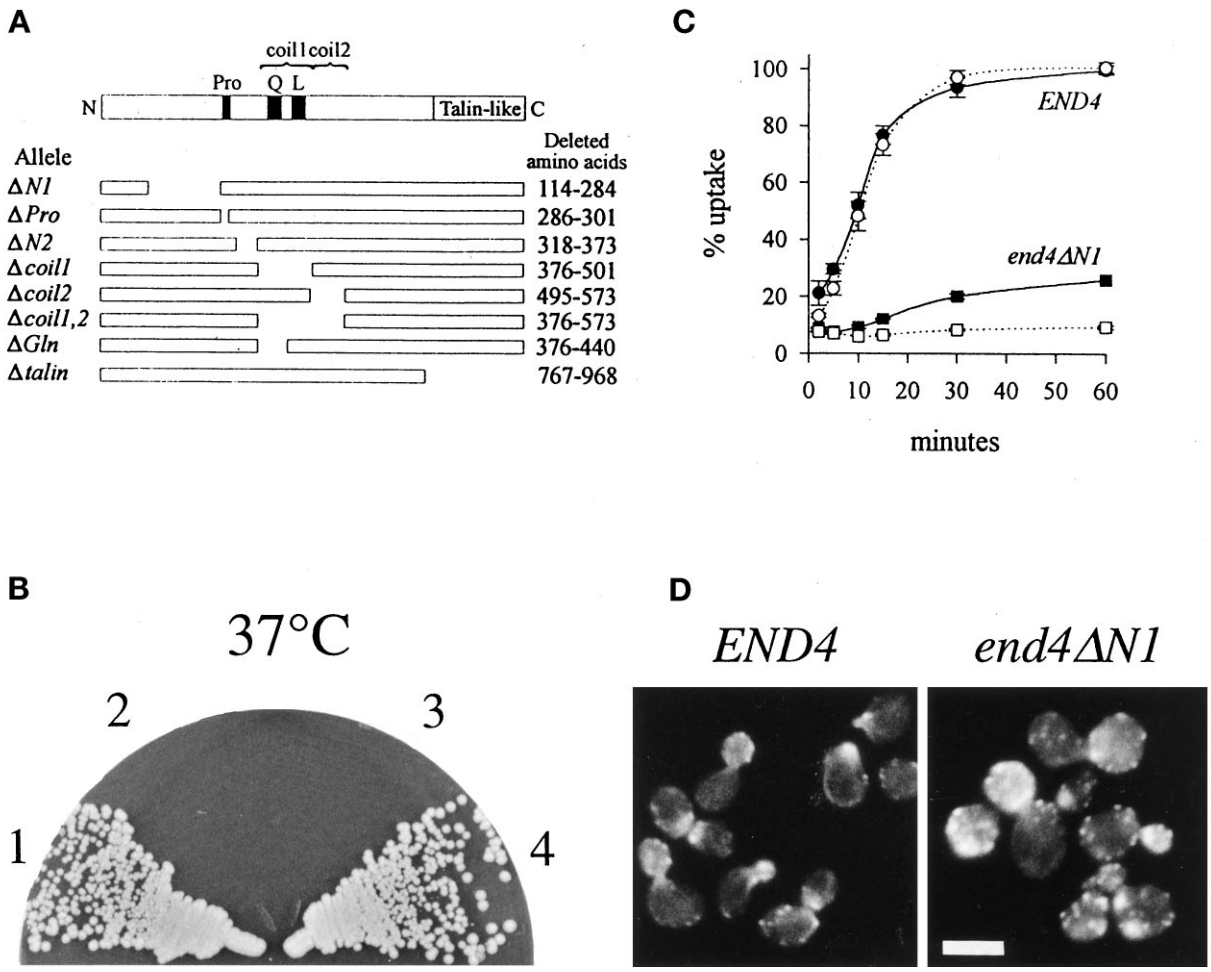

Figure 3. N terminus of End4p is essential for actin organization and endocytosis. (A) Mutant *end4* alleles devoid of the indicated regions (open space in the schematic representation) were generated as described in MATERIALS AND METHODS. Pro, proline-rich sequence; Q, glutamine-rich sequence; L, putative leucine-zipper; coil1 and coil2, putative coiled-coil regions 1 and 2, respectively. Proline at aa 498 divides the region from aa 376 to aa 573 into two separate coiled-coil domains (MATERIALS AND METHODS). The nomenclature of *end4* alleles and the deleted amino acids are indicated. (B) *END4* (section 1, RH3393), *end4*Δ (section 2, RH3212), *end4*Δ*N1* (section 3, RH3769), and *end4*Δ*coil1* (section 4, RH3395) strains were streaked onto YPUADT plates and incubated for 2 d at 37°C. Deletion of the N-terminal part of End4p but not deletion of the coiled-coil domain impairs growth at higher temperatures. (C) Receptor-mediated endocytosis of radiolabeled pheromone in *END4* (RH3393) and *end4*Δ*N1* (RH3769) strains after a 5-min preincubation at either 24°C (solid symbols) or 37°C (open symbols). (D) *END4* (RH3393) and *end4*Δ*N1* (RH3769) strains were grown at 24°C and processed for visualization of filamentous actin with rhodamine-conjugated phalloidin as described in MATERIALS AND METHODS. Bar, 5 μm.

*end4*Δ*xy* gene products were stably expressed at levels comparable to wild-type End4p, and we found that all mutant *end4* alleles could fully rescue the low spore viability of *end4*Δ segregants (our unpublished results). However, *end4*Δ*N1* mutants carrying a deletion in the N-terminal part of End4p could not grow at 37°C, whereas other *end4* mutants did not display any growth defect (Figure 3B; our unpublished observations). Thus, except for the N-terminal region, large parts of End4p including the coiled-coil domain and the talin-like region can be deleted without affecting growth.

All of the previously tested *end4* alleles displayed a temperature-dependent endocytosis defect (Raths *et al.*, 1993; Munn *et al.*, 1995; see above) and *end4*Δ mutants are defective for endocytosis even at their permissive growth temperature (Figure 1). To determine whether any of the deleted regions of End4p are required for endocytosis, we measured internalization of radiolabeled pheromone. The endocytic rates were expressed as a percentage of the wild-type internalization rate between 5 and 15 min after ligand addition. Strikingly, *end4*Δ*N1* mutants are defective for internalization of pheromone even at the permissive

Table 2. Endocytic rates

Strain	% wild-type rate
end4ΔN1	10
end4ΔN2	92
end4ΔPro	101
end4Δcoil1	108
end4ΔGln	68
end4Δcoil2	100
end4Δcoil1,2	69
end4Δtalin	98

Endocytic rates were calculated between 5 and 15 minutes after pheromone addition and expressed as a percentage of the wild-type endocytic rate. Strains used are listed in Table 1. Data shown is an average of at least two independent experiments. SD were less than 10%.

Table 3. Phenotypes of double mutants

Genotype	Growth 24°C	Growth 37°C	Actin 24°C	Endo 24°C
end4Δcoil1	+	+	+	+
abp1Δ	+	+	+	+
srv2Δ	+	−	ND	+
end4Δcoil1 abp1Δ	+	−	−	−
end4Δcoil1 abp1ΔSH3	+	−	ND	−
end4Δcoil1 srv2Δ	+	−	ND	−
end4Δcoil1 SRV2-5	+	+	ND	+

Summary of a subset of double mutants of *end4Δcoil1* and *abp1* or *srv2*, respectively. Growth was scored on YPUADT plates after 2 days (37°C) or 3 days (24°C) of incubation at the respective temperature. The actin cytoskeleton (Actin) was visualized with rhodamine-conjugated phalloidin as described. Endocytosis (Endo) of radiolabeled pheromone was measured as described. +, phenotype is identical, or very similar, to wild type; −, either no growth or a failure to properly polarize the actin cytoskeleton or a block in endocytosis, respectively; ND, not determined.

growth temperature of 24°C (Figure 3C), whereas all other *end4* mutants internalized α-factor with nearly wild-type kinetics at 24°C (Table 2). As for the growth requirement, large parts of End4p including the coiled-coil domain and the talin-like region can be deleted without affecting endocytosis.

END4/SLA2 is required for the organization and polarization of the actin cytoskeleton (Holtzman *et al.*, 1993). Because deletion of *END4* confers both a loss of actin organization and an endocytosis defect, we tested whether any of the newly generated *end4* alleles had an actin defect. Mutants were grown at 24°C and the actin cytoskeleton was visualized with rhodamine-conjugated phalloidin. Except for *end4ΔN1*, none of the *end4* mutants had an obvious actin defect at 24°C (Figure 3D; our unpublished observations). In *end4ΔN1* mutants, many actin patches were found in both mother and daughter cells, irrespective of the stage of the cell cycle, whereas in wild-type strains actin was polarized to actively growing regions in small buds. However, actin cables in *end4ΔN1* were similarly organized as in wild-type strains. Note that *end4ΔN1* mutants are larger and more spherical than wild-type counterparts. Thus, our results demonstrate that only the N-terminal domain of End4p is required for growth, actin organization, and endocytosis and that the coiled-coil region, the talin-like domain, the proline-rich region, and the Gln-rich region are apparently not essential for those processes.

Functional Overlap of the Coiled-Coil Region of End4p with ABP1 and SRV2 in Endocytosis

Because *end4 abp1Δ* double mutants are inviable (Holtzman *et al.*, 1993), we tested whether any of the newly generated *end4* deletion alleles caused inviability of an *abp1Δ* strain. Finding viable and lethal combinations of *end4Δxy abp1Δ* double mutants could help to correlate in vivo functions with different parts of End4p. We therefore crossed the *end4* deletion mutants to *abp1Δ* strains and analyzed double mutant segregants for growth on rich medium at 24°C and 37°C. We found that *end4ΔN1 abp1Δ* and *end4ΔGln abp1Δ* double mutants were inviable. Examination of those dissection plates showed that all predicted double mutants ceased growth after 2–10 cell divisions. All other combinations of *end4Δxy abp1Δ* double mutants were viable at 24°C (Table 3). However, in contrast to each single mutant, *end4Δcoil1 abp1Δ* and *end4Δcoil1,2 abp1Δ* double mutants were unable to grow at 37°C, whereas deletion of the proline-rich region, the talin-like domain, another domain in the N terminus, and deletion of the second coiled-coil domain of End4p in an *abp1Δ* background does not confer inviability at 37°C. To determine whether the coiled-coil region of End4p is required for organization of the actin cytoskeleton in addition to growth at high temperature in an *abp1Δ* background, we looked at the actin cytoskeleton in *end4Δcoil1 abp1Δ* mutants at their permissive growth temperature of 24°C. In wild-type cells and in *end4Δcoil1* and *abp1Δ* single mutants, actin cables traversing the mother cell and cortical actin concentrated in daughter cells could be seen (Figure 4A). In marked contrast, *end4Δcoil1 abp1Δ* double mutants have a strong defect in actin cytoskeleton organization and cells are larger and rounder than wild-type cells. Notably, the actin defect is similar to the one observed in *end4ΔN1* mutants, though in *end4Δcoil1 abp1Δ* mutants, the loss of polarization of actin patches is not as strong as in *end4ΔN1* mutants. Thus, in the absence of *ABP1*, deletion of the first coiled-coil domain of End4p results in a disorganized actin cytoskeleton at 24°C and impaired growth at 37°C. Because a defective actin cytoskeleton paralleled

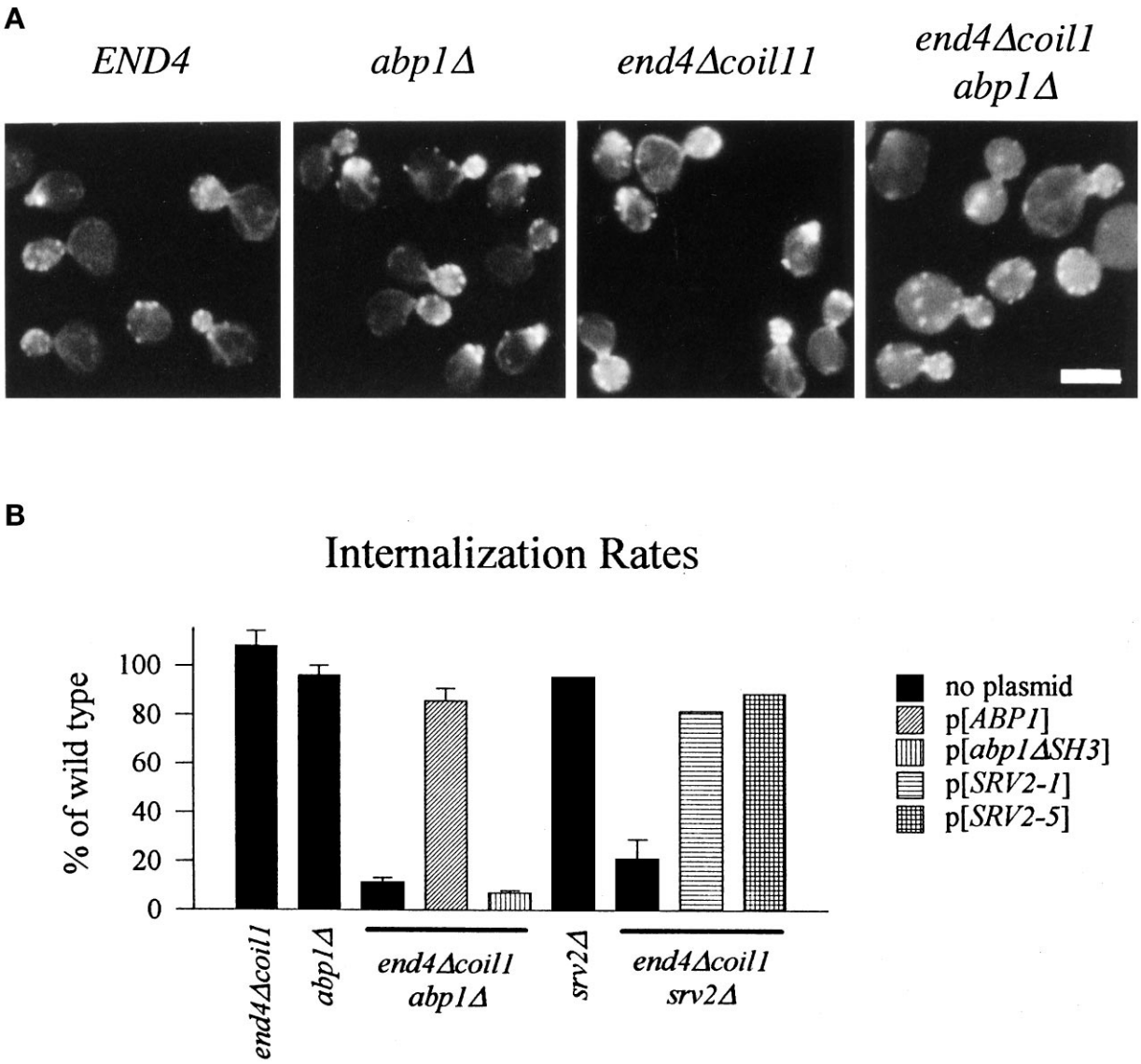

Figure 4. Abp1p and Srv2p have cryptic endocytic functions. (A) Visualization of filamentous actin with rhodamine-conjugated phalloidin of *END4* (RH3393), *abp1*Δ (RH3297), *end4*Δ*coil1* (RH3395), and *end4*Δ*coil1 abp1*Δ (RH3407) cells grown at 24°C. (B) Internalization rates expressed as a percentage of wild-type (RH3393) in *end4*Δ*coil1* (RH3395), *abp1*Δ (RH3297), and *srv2*Δ (RH4008) single mutants and in *end4*Δ*coil1 abp1*Δ (RH3407) or *end4*Δ*coil1 srv2*Δ (RH4009) double mutants transformed with the indicated plasmids, respectively. p[*abp1*Δ*SH3*] encodes a mutant allele of *ABP1* with a deleted SH3 domain; p[*SRV2–1*] encodes wild-type *SRV2* and p[*SRV2–5*] encodes a mutant allele of *SRV2* that lacks both binding sites for the SH3 domain of Abp1p. All plasmids are centromere-based and described in Lila and Drubin (1997).

the endocytosis defect in all *end4* mutants examined so far, we tested whether this was also true for the *end4*Δ*coil abp1*Δ double mutants by measuring endocytosis at 24°C. We calculated the amount of pheromone internalized per minute in the linear range of 5 to 15 min after pheromone addition and expressed this as a percentage of the wild-type endocytic rate. Both *end4*Δ*coil1* and *abp1*Δ single mutants internalized α-factor with wild-type kinetics (Figure 4B; Kübler and Riezman, 1993). Strikingly, deletion of the first coiled-coil domain of End4p in an *abp1*Δ background completely abolished endocytosis even at the permissive growth temperature of 24°C. As expected, the same effect was observed when both coiled-coil domains of End4p were deleted in the absence of *ABP1*, whereas combination of *end4*Δ*Pro*, *end4*Δ*N2*, *end4*Δ*coil2*, and *end4*Δ*talin* with *abp1*Δ did not significantly reduce endocytosis below the levels of the respective single mutants at any temperature (our unpublished observations). This strongly suggests that the coiled-coil domain of End4p mediates a function in endocytosis that is redundant with the function(s) of *ABP1*.

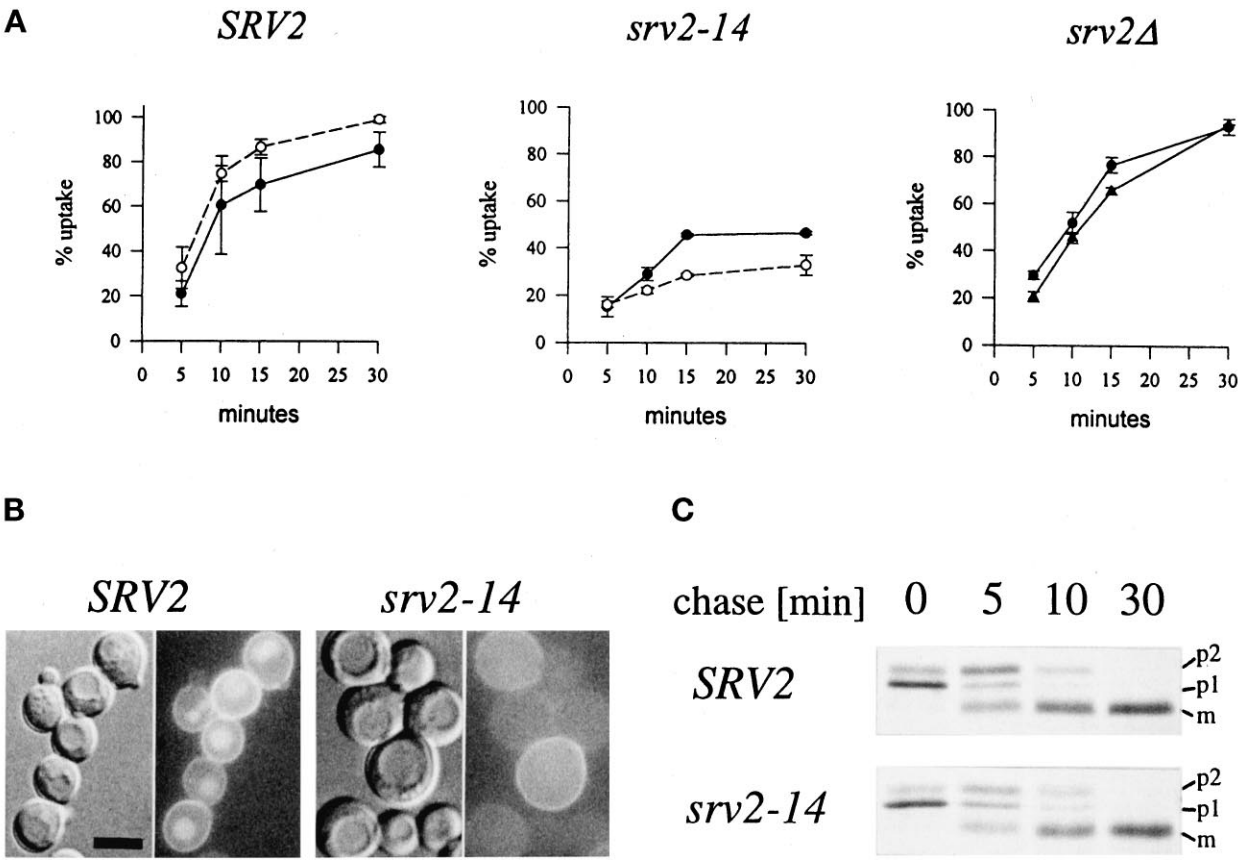

Figure 5. *srv2–14*, but not *srv2*Δ, mutations confer an endocytic defect. (A) Endocytosis of radiolabeled pheromone in *SRV2* (RH978) and *srv2–14* (RH3993) strains was measured at 24°C (solid symbols) or 37°C (open symbols) after a 15-min (*SRV2*, *srv2–14*) preincubation at the indicated temperature. Endocytosis in *srv2*Δ (RH4008, triangles) and *SRV2* (RH3393, circles) was measured after a 5-min preincubation at 24°C. (B) Accumulation of LY in *SRV2* (RH978) and *srv2–14* (RH3993) mutants grown at 24°C and preincubated for 15 min at 37°C prior to addition of LY for 1 h. (C) Maturation of radiolabeled CPY was measured in *SRV2* (RH978) and *srv2–14* (RH3993) mutants grown at 24°C and preincubated for 15 min at 37°C prior to starting a pulse–chase experiment as described in MATERIALS AND METHODS. p1, endoplasmic reticulum form of CPY; p2, Golgi-modified form of CPY; m, mature vacuolar form of CPY.

Using a previously described screen for endocytosis mutants (Munn and Riezman, 1994), we isolated a novel mutant, *end14–1*, that displays a temperature-sensitive growth phenotype. The endocytic defect of *end14–1* was tightly linked to impaired growth at 37°C through several back crosses, thus a single mutation caused both phenotypes. We used a CEN library to clone the wild-type *END14* gene by phenotypic complementation of the temperature-sensitive growth defect of an *end14–1* strain. Integrative mapping demonstrated that the cloned DNA encoded the authentic *END14* gene (MATERIALS AND METHODS). Mapping of the complementing ORF and sequence analysis revealed that *END14* is allelic to *SRV2*. From now on we refer to *end14–1* as *srv2–14*. At the permissive growth temperature of 24°C, *srv2–14* mutants are already quite defective for pheromone internalization and endocytosis of both α-factor and LY is completely blocked at 37°C (Figure 5, A and B). The *srv2–14* mutation therefore impairs both receptor-mediated and fluid-phase endocytosis. Surprisingly, deletion of *SRV2* did not confer an endocytosis defect (Figure 5A). This observation suggests that *srv2–14* is not a simple loss-of-function allele but acts in a recessive negative manner. To determine whether *srv2–14* mutants display a general defect in membrane transport, we followed the maturation of soluble vacuolar CPY. CPY is sequentially processed to its mature form because it is transported from the endoplasmic reticulum to the Golgi and finally to the vacuole. As shown in Figure 5C, CPY matures with wild-type kinetics in *srv2–14* mutants, even at the restrictive growth temperature of 37°C. These results show that *srv2–14* mutants are impaired in the internalization step of endocytosis but the early secretory pathway and the Golgi to vacuole transport steps remain unaffected.

Recently, Lila and Drubin (1997) showed a functional interaction of the SH3 domain of Abp1p and a

proline-rich sequence of Srv2p. We therefore tested whether the SH3 domain of Abp1p, and thus the binding of Abp1p to Srv2p, is required for the redundant endocytic function of Abp1p. As shown in Figure 4B, deletion of the SH3 domain of Abp1p in an *end4*Δ*coil1* background results in a complete loss of endocytosis at 24°C. This is consistent with the finding that Abp1p is required for endocytosis in the absence of the coiled-coil domain of End4p and it also demonstrates that the endocytic function of Abp1p depends on its SH3 domain. If binding of Abp1p via its SH3 domain to Srv2p were required for endocytosis in the *end4*Δ*coil1* mutant, one would expect that the absence of Srv2p or mutations in Srv2p that abolish binding of Srv2p to the SH3 domain of Abp1p would mimic the *end4*Δ*coil1 abp1*Δ*SH3* endocytosis defect if combined with an *end4*Δ*coil1* mutation. We therefore measured endocytosis of α-factor in strains carrying both the *end4*Δ*coil1* mutation and a deletion of *SRV2* or a deletion of the Abp1p-binding sites of Srv2p (*SRV2–5*; Lila and Drubin, 1997). Even though strains lacking Srv2p (such as strains lacking Abp1p) had no measurable endocytosis defect (Figures 4B and 5A), endocytosis in *end4*Δ*coil1 srv2*Δ double mutants was completely blocked, very similar to the *end4*Δ*coil1 abp1*Δ double mutant. Surprisingly, *end4*Δ*coil1 SRV2–5* double mutants internalized pheromone almost as efficiently as wild-type strains (Figure 4B). This suggests that binding of Srv2p to Abp1p, and therefore the cortical localization of Srv2p (Lila and Drubin, 1997), is most likely not required for the cryptic endocytic function of Abp1p or Srv2p. Thus, these results show that the coiled-coil domain of End4p mediates an endocytic function that is redundant with the endocytic function(s) of Abp1p and Srv2p.

DISCUSSION

END4 has previously been shown to be required for the process of endocytosis. We used a mutational analysis of *END4* to correlate in vivo functions with regions of End4p and we found that two parts of End4p participate in endocytosis. One of them resides in the N-terminal region and is essential for endocytosis and actin organization. The other contains a coiled-coil domain of End4p that is required for partitioning of End4p into a proteinaceous complex. In addition, this domain mediates an endocytic function that is redundant with function(s) of *ABP1* and *SRV2*. On the basis of biochemical, functional, and genetic data, we propose that *END4* may control endocytosis through the interaction with other actin-associated proteins (Figure 6).

A deletion of the N-terminal domain of End4p completely abolished endocytosis. In addition, *end4*Δ*N1* mutants display a loss of actin organization. Moreover, an actin defect always paralleled an endocytic

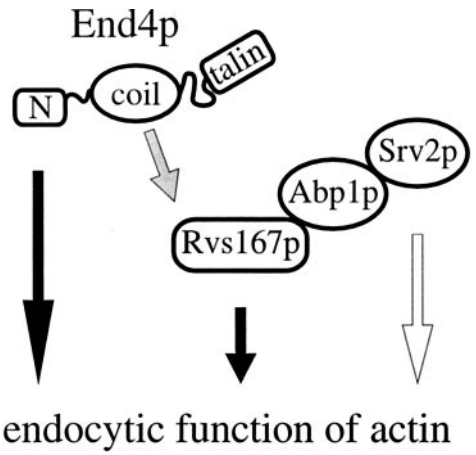

Figure 6. Hypothetical model. Two parts of End4p participate in endocytosis: the N terminus, which is essential for endocytosis and actin organization, and the coiled-coil domain, which mediates an endocytic function redundant with Abp1p and Srv2p. We propose that this function involves binding to Rvs167p, a protein itself required for endocytosis. The shaded arrow indicates that the physical interaction of End4p and Rvs167p is based solely on two-hybrid data. The open arrow indicates that a recessive negative mutation but not a deletion of *SRV2* results in a defect in endocytosis (see text for further explanations).

defect of *end4* mutants, suggesting that an actin-related function of End4p is essential for endocytosis. However, it is unlikely that *end4*Δ*N1* is a true *end4* null allele for the following reasons. First, the mutant allele fully complemented the germination defect of a null allele. Second, the mutant protein is stably expressed, and third, *end4*Δ*N1* mutants grow faster and reach higher density in stationary-phase cultures than *end4*Δ mutants (our unpublished observations). Perhaps the N-terminal part of End4p interacts with another protein(s) to mediate correct localization or maintenance of actin structures that may be a prerequisite for endocytosis. In support of this idea End4p stimulates polarized actin polymerization in vitro (Li *et al.*, 1995) and the talin-like domain of End4p was shown to be sufficient for interaction with actin filaments (McCann and Craig, 1997). The fact that deletion of this talin-like domain of End4p has no impact on endocytosis and actin organization suggests that either this function is not required for endocytosis or that other protein(s) could substitute for this loss of function.

Deletion of a central coiled-coil domain of End4p results in failure to partition into a proteinaceous complex. Furthermore, the absence of this region creates a synthetic endocytic defect in the absence of Abp1p or Srv2p. Thus, deletion of the coiled-coil domain of End4p clearly results in different phenotypes than those that are associated with an *end4*Δ*N1* allele. Consistent with this, *end4*Δ*N1 abp1*Δ double mutants are inviable whereas *end4*Δ*coil abp1*Δ double mutants are viable. It is therefore possible that the coiled-coil do-

main is functionally different from the N-terminal region of End4p. On the basis of our results, we propose that *END4*, *ABP1*, and *SRV2* have an overlapping endocytic function that is mediated through the coiled-coil domain of End4p. Consistent with this, deletion of the coiled-coil domain of End4p or deletion of *ABP1* or *SRV2* does not produce an obvious endocytic defect. However, combined deletions of the coiled-coil domain of End4p and deletion of *ABP1* (or its SH3 domain) or deletion of *SRV2* lead to a complete endocytosis defect, supporting the view of a common function of End4p, Abp1p, and Srv2p.

Abp1p (via its SH3 domain) binds to proline-rich sequences of Srv2p (Lila and Drubin, 1997) and both Abp1p or Srv2p are required for the redundant endocytic function with End4p. We therefore asked, whether an association of Srv2p with Abp1p was required for their endocytic function. The answer, however, is still ambiguous. Whereas deletion of the proline-rich sequences of Srv2p did not abrogate endocytosis in an *end4*Δ*coil1* mutant, deletion of the SH3 domain of Abp1p completely blocked endocytosis in an *end4*Δ*coil1* mutant. It could be that deletion of the SH3 domain of Abp1p is more deleterious to the physical interaction of Abp1p and Srv2p in vivo than deletion of the proline-rich sequences of Srv2p. Or as proposed (Lila and Drubin, 1997), the SH3 domain of Abp1p could bind other proteins in addition to Srv2p. It could be that one of those proteins is required for endocytosis in an *end4*Δ*coil1* mutant.

What could the common function of End4p, Abp1p, and Srv2p be? We speculate that it involves contacting Rvs167p. It has been shown that Abp1p binds to Rvs167p and that Abp1p provides a physical connection between Srv2p and Rvs167p. Interestingly, initial two-hybrid analysis indicates that the coiled-coil domain of End4p interacts with Rvs167p (Lombardi, unpublished observations). Consistent with this hypothesis that the common and essential function for endocytosis of the coiled-coil region of End4p, Abp1p, and Srv2p may be a physical connection to Rvs167p is the finding that Rvs167p is essential for endocytosis (Munn *et al.*, 1995). Alternatively, Abp1p and other proteins may be required for their mutual localization to perform their function(s). Failure to properly localize Rvs167p, Rvs161p, and Srv2p in *abp1*Δ strains could be the reason why *end4 abp1* double mutants are inviable. Consistent with this view, combined null alleles of *end4 rvs167*, *end4 rvs161*, and *end4 srv2* double mutants are inviable, although Abp1p is present. It could therefore be that the synthetic effects observed with the End4p coiled-coil mutant and *abp1* or *srv2* reflect partial effects on two distinct functions, one mediated by End4p and the other mediated by Rvs167p.

SRV2 has been isolated genetically as a gene required for RAS-mediated activation of the adenylate cyclase pathway and biochemically as an adenylate cyclase associated protein (Fedor-Chaiken *et al.*, 1990; Field *et al.*, 1990). However, *SRV2* has functions that are clearly not related to the RAS/adenylyl cyclase pathway and it was shown that Srv2p independently integrates RAS function and regulates the actin cytoskeleton organization (Field *et al.*, 1990; Gerst *et al.*, 1991). Most recently, Freeman *et al.* (1996) demonstrated that Srv2p binds to Abp1p independently of its cyclase association or actin-binding function. We report herein the isolation of a novel endocytosis mutant, *srv2–14*. It is likely that the recessive negative *srv2–14* mutation interferes with endocytosis by disrupting an actin-related function because actin is known to be required for endocytosis and because mutations that either increase or decrease the activity of adenylate cyclase do not affect endocytosis (Zanolari and Riezman, unpublished observations). How could it do this? It could be that Srv2–14p can enter into a protein complex and modify its function. As Srv2p is known to bind Abp1p, perhaps it binds Abp1p in such a manner that it can no longer release Rvs167p. This would sequester Rvs167p, which is strictly required for endocytosis. In this case, one would have to postulate that the wild-type Srv2p would successfully compete with the mutant Srv2–14p for binding to Abp1p, otherwise the mutation would be dominant. A complete loss of function of *SRV2* would not block endocytosis because the affinity of Abp1p for Rvs167p would not be increased. In the future it will be interesting to characterize this novel mutant *srv2–14* protein and its interactions with other actin-associated proteins.

ACKNOWLEDGMENTS

Susan Raths and Grace Parraga are acknowledged for the initial cloning of the *end4–1* complementing fragment. We are grateful to David Drubin and Tom Lila for providing strains and plasmids. We thank Mark Schönbächler for helpful comments on the manuscript. Nicolas Stern is acknowledged for technical assistance and many thanks go to Stephan Schröder for his valuable advice on centrifugation experiments. Very special thanks go to Maribel Geli for stimulating discussions, helpful suggestions, and critical comments throughout the progression of this work. Markus Wenk is acknowledged for culinary delights and conversation that improved life outside the laboratory substantially. We thank P. James and R. Sternglanz for the two-hybrid vectors and strain. This work was funded by the Canton of Basel Stadt and by a grant to H.R. from the Swiss National Science Foundation.

REFERENCES

Adams, A.E., and Pringle, J.R. (1984). Relationship of actin and tubulin distribution to bud growth in wild type and morphogenetic mutant *Saccharomyces cerevisiae*. J. Cell Biol. *98*, 934–945.

Allen, L.H., and Aderem, A. (1995). A role for MARCKS, the alpha isozyme of protein kinase C and myosin I in zymosan phagocytosis by macrophages. J. Exp. Med. *182*, 829–840.

Bauer, F., Urdaci, M., Aigle, M., and Crouzet, M. (1993). Alteration of a yeast SH3 protein leads to conditional viability with defects in cytoskeletal and budding patterns. Mol. Cell. Biol. *13*, 5070–5084.

Bénédetti, H., Raths, S., Crausaz, F., and Riezman, H. (1994). The *END3* gene encodes a protein that is required for the internalization step of endocytosis and for actin cytoskeleton organization in yeast. Mol. Biol. Cell *5*, 1023–1037.

Burridge, K., Fath, K., Kelly, T., Nuckolls, G., and Turner, C. (1988). Focal adhesions: transmembrane junctions between the extracellular matrix and the cytoskeleton. Annu. Rev. Cell Biol. *4*, 487–525.

Chenevert, J., Corrado, K., Bender, A., Pringle, J., and Herskowitz, I. (1992). A yeast gene (*BEM1*) necessary for cell polarization whose product contains two SH3 domains. Nature *356*, 77–79.

Crouzet, M., Urdaci, M., Dulau, L., and Aigle, M. (1991). Yeast mutant affected for viability upon nutrient starvation: characterization and cloning of the *RVS161* gene. Yeast *7*, 727–743.

David, C., McPerson, P.S., Mundigl, O., and De Camilli, P. (1996). A role of amphiphysin in synaptic vesicle endocytosis suggested by its binding to dynamin in nerve terminals. Proc. Natl. Acad. Sci. USA *93*, 331–335.

Drubin, D.G., Miller, K.G., and Botstein, D. (1988). Yeast actin-binding proteins: evidence for a role in morphogenesis. J. Cell Biol. *107*, 2551–2561.

Drubin, D.G., Mulholland, J., Zhu, Z.M., and Botstein, D. (1990). Homology of a yeast actin-binding protein to signal transduction proteins and myosin-I. Nature *343*, 288–290.

Dulic, V., Egerton, M., Elguindi, I., Raths, S., Singer, B., and Riezman, H. (1991). Yeast endocytosis assays. Methods Enzymol. *194*, 697–710.

Fedor-Chaiken, M., Deschenes, R.J., and Broach, J.R. (1990). *SRV2*, a gene required for *RAS* activation of adenylate cyclase in yeast. Cell, *61*, 329–340.

Field, J., Vojtek, A., Ballester, R., Bolger, G., Colicelli, J., Ferguson, K., Gerst, J., Kataoka, T., Michaeli, T., Powers, S., Riggs, M., Rodgers, L., Wieland, I., Wheland, B., and Wigler, M. (1990). Cloning and characterization of CAP, the *S. cerevisiae* gene encoding the 70kd adenylyl cyclase-associated protein. Cell *61*, 319–327.

Fields, S., and Sternglanz, R. (1994). The two-hybrid system: an assay for protein-protein interactions. Trends Genet. *10*, 286–292.

Freeman, N.L., Chen, Z., Horenstein, J., Weber, A., and Field, J. (1995). An actin monomer binding activity localizes to the carboxyl-terminal half of the *Saccharomyces cerevisiae* cyclase-associated protein. J. Biol. Chem. *270*, 5680–5685.

Freeman, N.L., Lila, T., Mintzer, K.A., Cgen, Z., Pahk, A.J., Ren, R., Drubin, D.G., and Field, J. (1996). A conserved proline-rich region of the *Saccharomyces cerevisiae* cyclase-associated protein binds SH3 domains and modulates cytoskeletal localization. Mol. Cell. Biol. *16*, 548–556.

Geli, M., and Riezman, H. (1996). Role of type I myosins in receptor-mediated endocytosis in yeast. Science *272*, 533–535.

Gerst, J.E., Ferguson, K., Vojtek, A., Wigler, M., and Field, J. (1991). CAP is a bifunctional component of the *Saccharomyces cerevisiae* adenylyl cyclase complex. Mol. Cell. Biol. *11*, 1248–1257.

Greenberg, S., Burridge, K., and Silverstein, S.C. (1990). Colocalization of F-actin and talin during Fc receptor-mediated phagocytosis in mouse macrophages. J. Exp. Med. *172*, 1853–1856.

Griffith, O.M. (1979). Techniques of preparative, zonal, and continuous flow ultracentrifugation. Fullerton, CA: Applications Research Department Spinco Division, Beckman Instruments.

Harbury, P.B., Zhang, T., Kim, P.S., and Alber, T. (1993). A switch between two-, three-, and four-stranded coiled coils in GCN4 leucine zipper mutants. Science *262*, 1401–1407.

Harlow, E., and Lane, D. (1988). Antibodies: A Laboratory Manual, Cold Spring Harbor, NY: Cold Spring Harbor Laboratory Press.

Hicke, L., Zanolari, B., Pypaert, M., Rohrer, J., and Riezman, H. (1997). Transport through the yeast endocytic pathway occurs through morphologically distinct compartments and requires an active secretory pathway and Sec18p/*N*-ethylmaleimide-sensitive fusion protein. Mol. Biol. Cell *8*, 13–31.

Holtzman, D.A., Yang, S., and Drubin, D.G. (1993). Synthetic-lethal interactions identify two novel genes, *SLA1* and *SLA2*, that control membrane cytoskeleton assembly in *Saccharomyces cerevisiae*. J. Cell Biol. *122*, 635–644.

Horvath, A., and Riezman, H. (1994). Rapid protein extraction from *Saccharomyces cerevisiae*. Yeast *10*, 1305–1310.

Kübler, E., and Riezman, H. (1993). Actin and fimbrin are required for the internalization step of endocytosis in yeast. EMBO J. *12*, 2855–2862.

Kübler, E., Schimmöller, F., and Riezman, H. (1994). Calcium-independent calmodulin requirement for endocytosis in yeast. EMBO J. *13*, 5539–5546.

Li, R., Zheng, Y., and Drubin, D.G. (1995). Regulation of cortical actin cytoskeleton assembly during polarized cell growth in budding yeast. J. Cell Biol. *128*, 599–615.

Lila, T., and Drubin, D. (1997). Evidence for physical and functional interactions among two *Saccharomyces cerevisiae* SH3 domain proteins, an adenylyl cyclase-associated protein and the actin cytoskeleton. Mol. Biol. Cell *8*, 367–385.

Luna, E.J. (1991). Molecular links between the cytoskeleton and membranes. Curr. Opin. Cell Biol. *3*, 120–126.

McCann, R.O., and Craig, S.W. (1997). The I/LWEQ module: a conserved sequence that signifies F-actin binding in functionally diverse proteins from yeast to mammals. Proc. Natl. Acad. Sci. USA *94*, 5679–5684.

Miller, J.H. (1972). Experiments in Molecular Genetics. Cold Spring Harbor, NY: Cold Spring Harbor Laboratory Press, 352–355.

Muguruma M., Matsumura S., and Fukazawa T. (1990). Direct interactions between talin and actin. Biochem. Biophys. Res. Commun. *171*, 1217–1223.

Mulholland, J., Preuss, D., Moon, A., Wong, A., Drubin, D., and Botstein, D. (1994). Ultrastructure of the yeast actin cytoskeleton and its association with the plasma membrane. J. Cell Biol. *125*, 381–391.

Mulholland, J., Wesp, A., Riezman, H., and Botstein, D. (1997). Yeast actin cytoskeleton mutants accumulate a new class of Golgi-derived secretory vesicles. Mol. Biol. Cell *8*, 1481–1499.

Munn, A.L., and Riezman, H. (1994). Endocytosis is required for the growth of vacuolar H+-ATPase-defective yeast: identification of six new *END* genes. J. Cell Biol. *127*, 373–386.

Munn, A.L., Stevenson, B.J., Geli, M.I., and Riezman, H. (1995). *end5, end6,* and *end7*: mutations that cause actin delocalization and block the internalization step of endocytosis in *Saccharomyces cerevisiae*. Mol. Biol. Cell *6*, 1721–1742.

Na, S., Hincapie, M., McCusker, J.H., and Haber, J.E. (1995). *MOP2* (*SLA2*) affects the abundance of the plasma membrane H^+-ATPase of *Saccharomyces cerevisiae*. J. Biol. Chem. *270*, 6815–6823.

Pollard, T.D., Almo, S., Quirk, S., Vinson, V., and Lattman, E.E. (1994). Structure of actin binding proteins: insights about function at atomic resolution. Annu. Rev. Cell Biol. *10*, 207–249.

Pryer, N.K., Salama, N.R., Schekman, R., and Kaiser, C.A. (1993). Cytosolic Sec13p complex is required for vesicle formation from the endoplasmic reticulum in vitro. J. Cell Biol. *120*, 865–875.

Raths, S., Rohrer, J., Crausaz, F., and Riezman, H. (1993). *end3* and *end4*: two mutants defective in receptor-mediated and fluid-phase endocytosis in *Saccharomyces cerevisiae*. J. Cell Biol. *120*, 55–65.

Rees, D.J.G., Ades, S.E., Singer, S.J., and Hynes, R.O. (1990). Sequence and domain structure of talin. Nature *347*, 685–689.

Ren, R., Mayer, B.J., Cichette, P., and Baltimore, D. (1993). Identification of a ten-amino acid proline-rich SH3 binding site. Science *259*, 1157–1161.

Rose, M.D., Novick, P., Thomas, J.H., Botstein, D., and Fink, G.R. (1987). A *Saccharomyces cerevisiae* genomic plasmid bank based on a centromere-containing shuttle vector. Gene *60*, 237–243.

Sambrook, J., Fritsch, E.F., and Maniatis, T. (1989). Molecular Cloning: A Laboratory Manual, 2nd ed., Cold Spring Harbor, NY: Cold Spring Harbor Laboratory Press.

Schimmöller, F., Singer-Krüger, B., Schröder, S., Krüger, U., Barlowe, C., and Riezman, H. (1995). The absence of Emp24p, a component of ER-derived COPII-coated vesicles, causes a defect in transport of selected proteins to the Golgi. EMBO J. *14*, 1329–1339.

Schröder, S., Schimmöller, F., Singer-Krüger, B., and Riezman, H. (1995). The Golgi-localization of yeast Emp47p depends on its Di-lysine motif but is not affected by the *ret1–1* mutation in α-COP. J. Cell Biol. *131*, 895–912.

Sherman, F., Fink, G., and Lawrence, C. (1974). Methods in Yeast Genetics, Cold Spring Harbor, NY: Cold Spring Harbor Laboratory Press.

Sikorski, R.S., and Hieter, P. (1989). A system of shuttle vectors and yeast host strains designed for efficient manipulation of DNA in *Saccharomyces cerevisiae*. Genetics *122*, 19–27.

Sivadon, P., Bauer, F., Aigle, M., and Crouzet, M. (1995). Actin cytoskeleton and budding pattern are altered in the yeast *rvs161* mutant: the Rvs161 protein shares common domains with the brain protein amphiphysin. Mol. Gen. Genet. *246*, 485–495.

Turner, C.E., and Burridge, K. (1991). Transmembrane molecular assemblies in cell-extracellular matrix interactions. Curr. Opin. Cell Biol. *3*, 849–853.